Vietnam Journal of Marine Science and Technology 2025, 25(4) 405–417

Vietnam Academy of Science and Technology

Vietnam Journal of Marine Science and Technology

journal homepage: vjs.ac.vn/index.php/jmst

Application of the MIKE 21/3 coupled model to simulate the hydrodynamic regime in the Tra Khuc River Estuary, Quang Ngai Province

Dao Dinh Cham[1,2], Ganzey Kirill[3], Dao Thi Thao[1], Dang Thi Hong Nhung[1], Hoang Thai Binh[1,2,*]

[1]*Institute of Earth Sciences, VAST, Vietnam*
[2]*Graduate University of Science and Technology, VAST, Vietnam*
[3]*Pacific Institute of Geography, Far Eastern Branch, Russian Academy of Sciences, Vladivostok, 690041 Russia*

Received: 2 October 2025; Accepted: 14 November 2025

ABSTRACT

This study applies the MIKE 21/3 Couple model to simulate the hydrodynamic regime of the Tra Khuc River estuary. The model was calibrated and validated using observed water level and wave data from the study area, with evaluation metrics indicating good performance. Simulations were carried out for two monsoon scenarios (Southwest and Northeast). The results show that during the Southwest monsoon, the current mainly flows along the shoreline from south to north, with an average velocity of about 0.05–0.15 m/s; average wave height in offshore areas is greater than 0.8m, while in the estuary it ranges from 0.2 to 0.4 m. During the Northeast monsoon, both current velocities and wave heights are higher compared to the Southwest monsoon. The average current velocity is 0.05–0.25 m/s, flowing from north to south, and offshore wave heights range from 3.6 to 4.0 m, with some areas exceeding 4.0 m. The findings provide an essential scientific basis for sediment transport assessment and for developing coastal management and planning strategies in Quang Ngai Province.

Keywords: Hydrodynamics, Tra Khuc estuary, MIKE 21/3 model.

[*]Corresponding author at: Institute of Earth Sciences, 68 Huynh Thuc Khang Street, Lang Ward, Hanoi City, Vietnam.
E-mail addresses: binhht060774@gmail.com

https://doi.org/10.15625/1859-3097/23573

Introduction

Coastal estuaries represent crucial transitional zones between river and marine systems, where complex dynamic processes such as river flow, tides, waves, winds, and sediment transport simultaneously interact. These processes govern the formation and morphological evolution of estuaries, directly influencing coastal ecosystems and socio-economic activities. In the context of climate change, sea-level rise, and increasing coastal exploitation, the hydrodynamic regime in estuarine areas has become more complex and variable. It poses risks of abnormal erosion and accretion, threatening sustainable coastal development.

Over the past decades, numerous international studies have applied numerical models to analyze and predict hydrodynamic regimes and estuarine morphological evolution [1–13]. Models such as Delft3D [7, 14–16], ROMS [17–19], and MIKE [20, 21] have been widely employed to simulate flow fields, wave dynamics, and sediment transport. These studies have demonstrated the capability of numerical models to explain wave–current interactions, forecast erosion–accretion trends, and support coastal resource management. In Vietnam, several studies have applied advanced hydrodynamic models to major estuaries, including the Hai Phong coastal area [22], the coastal area of Da Nang [23–25], the Mekong Delta estuarine system [26, 27], the Nhat Le estuary [28, 29], the Da Nong estuary [30], the Co To coastal zone [31], coastal estuaries in the Ma River basin [32], and the Dai estuary [33]. Their results have provided valuable scientific foundations for coastal management, planning, and protection.

The Tra Khuc estuary is the largest in Quang Ngai Province, with a catchment area exceeding 3.000 km², discharging into the sea at the Co Luy estuary (Fig. 1). The estuarine topography consists of the main channel, tidal flats, and sandbars; the area is influenced by an irregular semidiurnal tide (tidal range 1.5–2.0 m), the Northeast and Southwest monsoons, and river floods during the rainy season. The interaction of these factors results in complex hydrodynamic variations, causing irregular erosion and accretion that affect navigation channels, seaports, residents, and coastal production activities.

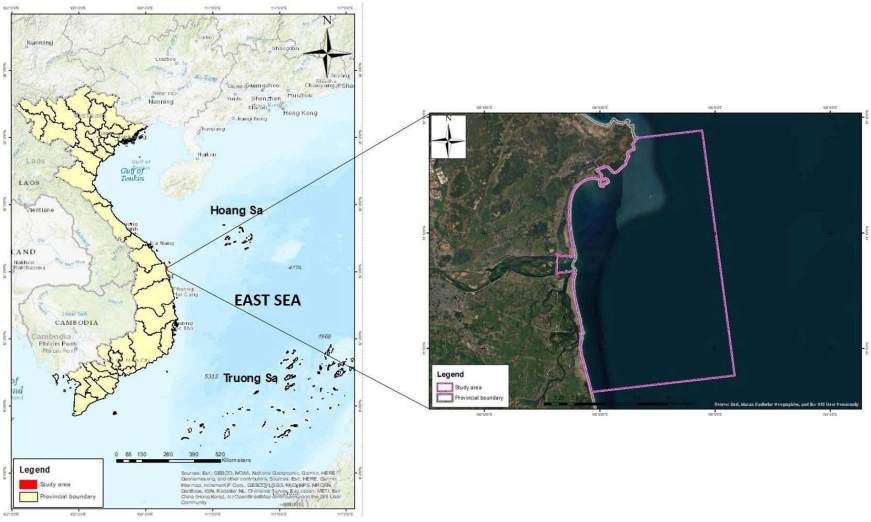

Figure 1. Study area

Although the Tra Khuc estuary holds significant scientific and practical importance, studies applying the MIKE 21/3 Coupled model to simulate its hydrodynamic regime remain limited. Most previous studies have focused mainly on qualitative assessments and have not comprehensively analyzed seasonal hydrodynamic variations under different monsoon conditions. Therefore, there is a need for a modern modeling approach that ensures

scientific rigor while serving practical management purposes.

This study applies the MIKE 21/3 Coupled model (integrating MIKE 21-FM and MIKE 21-SW) to simulate the hydrodynamic regime of the Tra Khuc estuary under two monsoon scenarios: Northeast and Southwest. The objectives are to establish and validate the model using topographic, water-level, wave, and wind data; analyze hydrodynamic characteristics under monsoon conditions; and provide a scientific basis for sediment transport assessment, morphological change analysis, and sustainable coastal development planning for Quang Ngai Province.

Database and Research Methods

Data Use

Topographic data of the river area at a scale of 1/10,000, and the offshore sea area at a scale of 1/50,000 were inherited from previous research projects combining topographic data surveyed in the estuary and the coastal regions of Tra Khuc river mouth, which was conducted by the Institute of Geography (now the Institute of Earth Sciences, Vietnam Academy of Science and Technology). The collected and surveyed topographic data were standardized to the WGS84 coordinate system and exported in *.xyz format to generate the computational mesh for the model (Fig. 2).

Wave and water level measurements at Stations A and B (Fig. 2) were surveyed during the periods from April 10–24, 2022, and March 18–25, 2023. These datasets were used for model calibration and validation.

Wave and wind data were obtained from the European Centre for Medium-Range Weather Forecasts (ECMWF) reanalysis and used as offshore boundary conditions and forcings for the model.

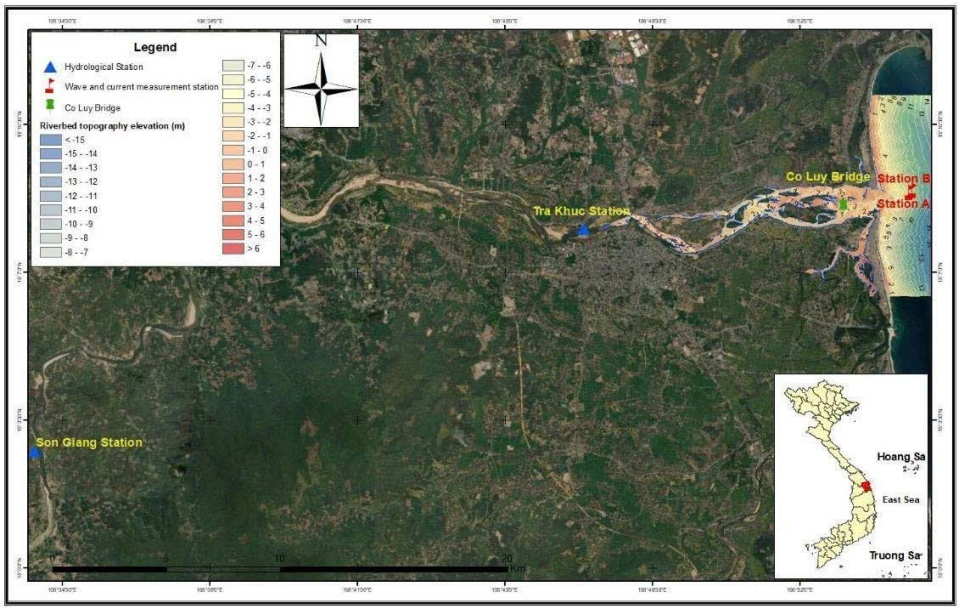

Figure 2. Topography of the Tra Khuc estuary area, Locations of wave and current measurement stations, location of river boundary extraction, and calibration/validation stations of the MIKE 11 model

Research Methods

In this study, the MIKE modeling system developed by the Danish Hydraulic Institute (DHI) was used to simulate the hydrodynamic regime of the Tra Khuc estuary. Specifically, the MIKE 11 hydrodynamic model was employed to calculate boundary conditions for the MIKE 21

model. The MIKE 21/3 Coupled Model, which integrates two modules - the MIKE 21FM hydrodynamic module and the MIKE 21SW wave module - was then used to simulate estuarine hydrodynamics. The interaction between waves and currents is better represented when the two modules are coupled.

The current and wave modules are the two fundamental components of the MIKE 21/3 FM Coupled Model.

MIKE 21 FM Hydrodynamic Module [34]: This is the core module used to calculate the current field based on a flexible, unstructured triangular mesh approach. It is widely applied in studies of oceanography and coastal - estuarine environments. The module is governed by two main equations: the continuity equation and the momentum equation.

MIKE 21 SW Spectral Wave Module [34]: This module calculates the wind-wave spectrum on an unstructured mesh. It simulates the generation, dissipation, and propagation of wind and swell waves in both offshore and nearshore regions.

Model setup, calibration, and validation

The construction of the computational mesh and the model setup are crucial steps in simulating hydrodynamic processes. The computational domain and mesh resolution determine the model's calculation time, stability, and result accuracy. The computational domain is centered on the Tra Khuc estuary and extends northward and southward along the coastline. The purpose of expanding the domain is to minimize boundary effects on the estuary area and to allow for the simulation of hydrodynamic characteristics on both sides of the coast. The northern boundary is located approximately 12 km from the estuary, the southern boundary about 12 km away, and the eastern (offshore) boundary roughly 6 km from the estuary (Fig. 3). The upstream river boundary extends to the Co Luy Bridge. The mesh is refined in the river and estuarine areas, with cell sizes ranging from 50 to 60 m, while in deeper offshore areas, the grid is sparser, with cell sizes ranging from 200 to 400 m.

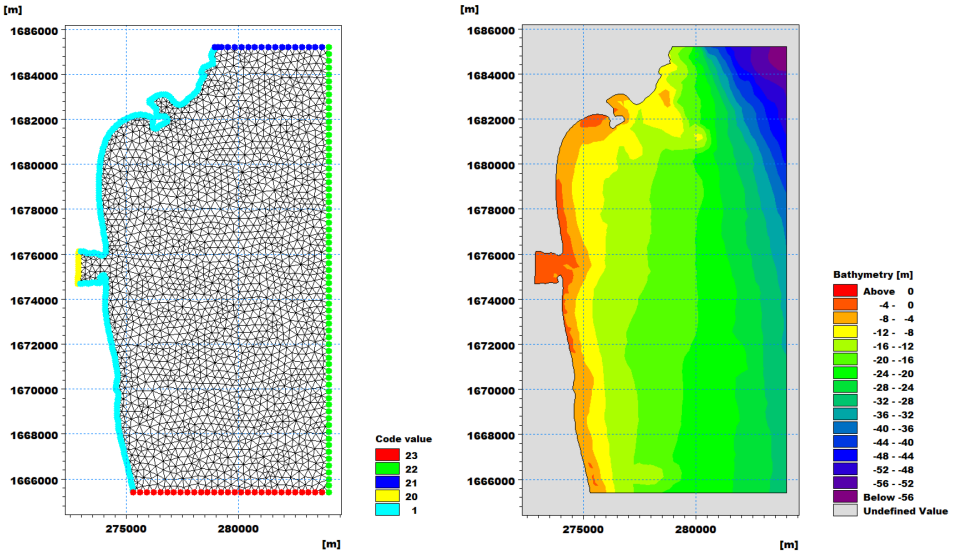

(a) Grid (b) Bathymetry

Figure 3. Computational grid and bathymetry of the study area

* Regarding boundary conditions for the hydrodynamic model:

- Northern, eastern, and southern boundaries: Tidal level data at these boundaries were extracted from the MIKE 21 Toolbox. Given the various studies on hydrodynamic modeling in coastal and estuarine regions of Vietnam, particularly in the central coastal areas [23, 28, 35], and considering that the study area is relatively small and less affected by the general

circulation of the East Sea, this study uses only tidal-level boundaries.

- Upstream river boundary: The river discharge data at the Co Luy Bridge were derived from the one-dimensional hydrodynamic model MIKE 11, which was established, calibrated, and validated for two flood events occurring from November 3–10, 2017, and from October 23–November 8, 2020. This model system was inherited from the project "Application of geospatial technology in developing models for natural hazard warning" (Project Code: CT0649.01/21–23) conducted by the Institute of Geography (now Institute of Earth Sciences), Vietnam Academy of Science and Technology.

Figure 4 presents the simulated and observed water levels during the MIKE 11 model calibration phase. At the Son Giang hydrological station, the simulated water level was 0.183 m lower than the observed water level. At the Tra Khuc hydrological station, the simulated water level is 0.113 m lower than the observed value. The Nash coefficients at the Son Giang and Tra Khuc stations are 0.85 and 0.92, respectively (Table 1).

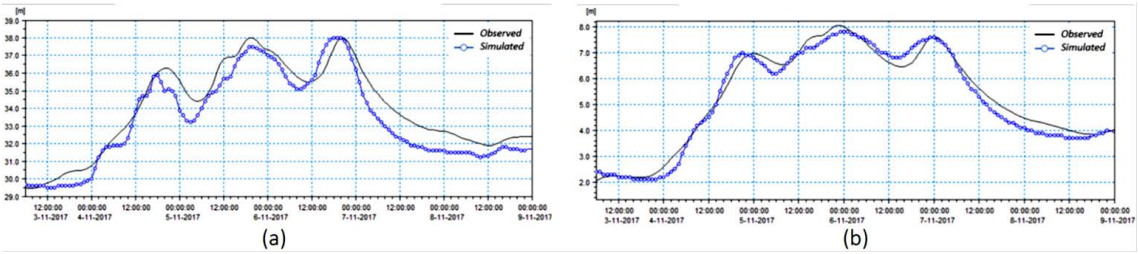

Figure 4. Comparison of simulated and observed water level hydrographs at stations (a) Son Giang and (b) Tra Khuc during the calibration period

Table 1. Error assessment results of the MIKE 11 model calibration and validation

	Station	H_{max} observed	H_{max} simulated	NSE
Calibration (03/11–10/11/2017)	Son Giang	37,990	37,807	0.85
	Tra Khuc	8,013	7,900	0.92
Validation (23/10–08/11/2020	Son Giang	38,710	38,722	0.88
	Tra Khuc	7,730	7,936	0.77

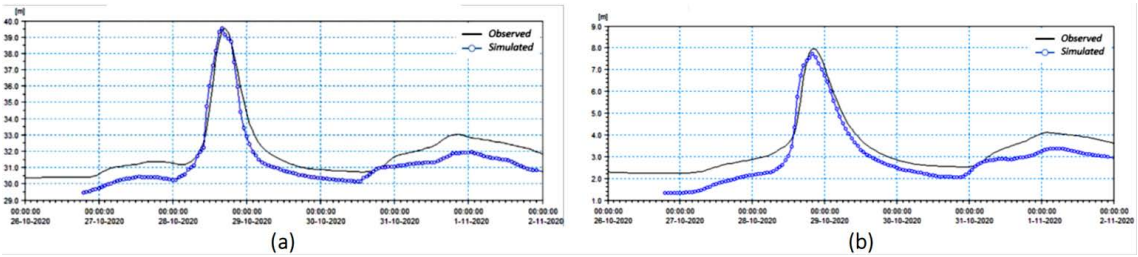

Figure 5. Comparison of simulated and observed water level hydrographs at stations (a) Son Giang and (b) Tra Khuc during the validation period

The validation results for the flood event from 23 October to 8 November 2020 are satisfactory. Figure 5 demonstrates the simulated and observed water levels during the inspection period. At the Son Giang hydrological station, the simulated water level (H_{sim} = 38.722 m) is 0.012 m higher than the observed value. At the Tra Khuc hydrological station, the simulated water level (H_{sim} = 7.936 m) is 0.206 m higher than the observed value. The Nash coefficients at the Son Giang and Tra Khuc stations are 0.80 and 0.77, respectively. Based on these results, it

can be concluded that the model satisfactorily reproduces the flood conditions of the Tra Khuc River system, and it can therefore be used to extract river discharge data as boundary inputs for the MIKE 21 model.

* Regarding the boundary conditions of the wave model:

- Wind data: The wind field across the entire computational domain was obtained from the ERA5 reanalysis dataset with a spatial resolution of 0.25°, downloaded from the European Centre for Medium-Range Weather Forecasts (ECMWF) (Link: https://cds.climate.copernicus.eu/datasets).

- Boundary conditions: The northern, southern, and upstream (river) boundaries were set as radiation boundaries, while the eastern (offshore) boundary used wave data from the European Centre for Medium-Range Weather Forecasts (ECMWF).

After model setup, calibration, and validation were carried out using observed water level, current, and wave data. The performance of the calibration and validation was evaluated using the Nash-Sutcliffe Efficiency (NSE) coefficient for water level and current data, and the Root Mean Square Error (RMSE) for wave parameters.

$$NSE = 1 - \frac{\sum_{i=1}^{n}\left(x_{obs} - x_{sim}\right)^2}{\sum_{i=1}^{n}\left(x_{obs} - \overline{x}_{obs}\right)^2} \quad (1)$$

$$RMSE = \sqrt{\frac{1}{2}\sum_{i=1}^{n}\left(x_{obs} - x_{sim}\right)^2} \quad (2)$$

where: x_{obs} is the observed value, x_{sim} is the simulated value from the model.

The model calibration was performed using observed wave and water level data from March 18–25, 2023, at Station A (Fig. 2).

The model calibration involved adjustments to the significant wave height, peak spectral period, wave direction, and water level (Fig. 6). The results indicate that the simulated wave height, period, and direction are in good agreement with the observed data, with an RMSE value of 0.05 (Table 2). The simulated and observed water levels show consistent phase and magnitude, with NSE coefficient of 0.92, indicating good agreement. These results demonstrate that the model accurately simulates hydrodynamic conditions. Therefore, the calibrated model parameters were retained for the validation phase, conducted from 10 April to 24 April, 2022.

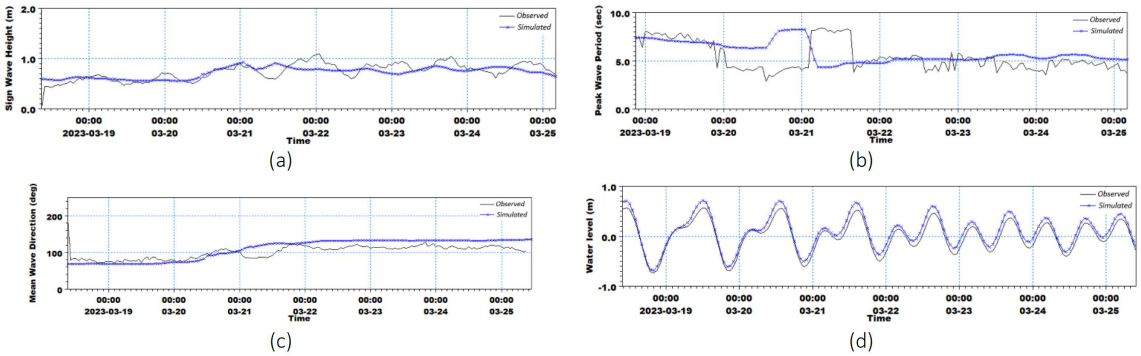

Figure 6. (a) Observed and simulated significant wave height; (b) Observed and simulated peak wave period; (c) Observed and simulated wave direction; (d) Observed and simulated water level at Station A during the calibration period

Table 2. Error assessment results of the model calibration

Station	Parameters	Time	*NSE*	*RMSE*
Station A	Wave height	18–25/3/2023		0.05
	Water level		0.92	

Model validation was performed using observed wave and water-level data from April 10–24, 2022, at Station B (Fig. 2).

Figure 7 presents the comparison between simulated and observed wave height, wave period, and wave direction at Station B during the validation period. The results show that the model performs well at the validation station, with good agreement between simulated and observed data (RMSE = 0.05) (Table 3). These results indicate that the model demonstrates high reliability with the set of parameters presented in Table 4. Therefore, the model can be applied to simulate the current and wave fields in the coastal and estuarine areas of the Tra Khuc River.

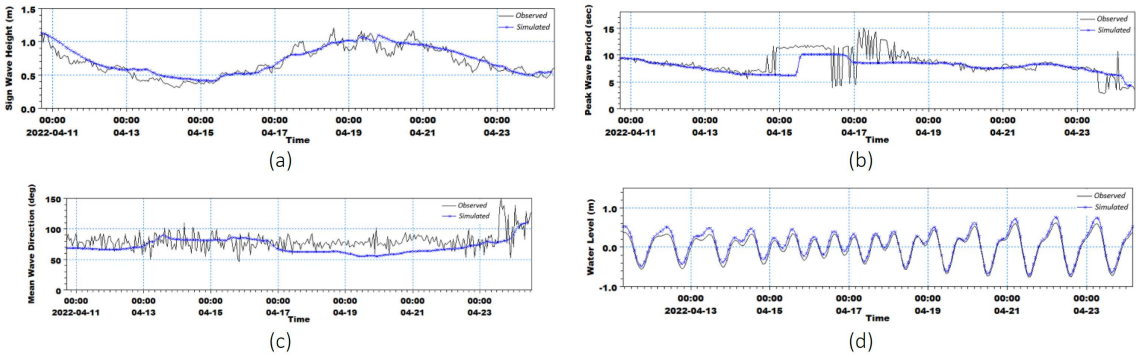

Figure 7. (a) Observed and simulated significant wave height; (b) Observed and simulated peak wave period; (c) Observed and simulated wave direction; (d) Observed and simulated water level at Station B during the validation period

Table 3. Error assessment results of the model validation

Station	Parameters	Time	*NSE*	*RMSE*
Station B	Wave height	10–25/09/2020		0.05
	Water level		0.93	

Table 4. Parameter set of the MIKE 21/3 Coupled Model

No.	Model parameter	Value
1	Bottom roughness coefficient	36
2	Wind friction coefficient	Defined according to the model's default formulation
3	Eddy viscosity coefficient	0.28
4	Convergence coefficient	5
5	Wave breaking coefficient	0.8
6	Horizontal diffusion ratio	1
7	Internal friction angle of sediment	30^{o}
8	Bottom friction coefficient	0.001

Scenario Development

To gain a comprehensive understanding of the hydrodynamic characteristics in the Tra Khuc estuary, the study constructed simulation scenarios for two main cases: the Northeast and the Southwest monsoons. The simulation periods were defined as follows: Northeast monsoon: from October to December 2022, Southwest monsoon: from June to August 2022. These months represent the two dominant monsoon seasons and are minimally affected by other weather systems. Boundary conditions-including tidal boundaries, river boundaries, wind fields, and offshore wave boundaries-were assigned consistently for each simulation period.

Results

Current and wave characteristics in the Northeast monsoon

During the Northeast monsoon period, the average current velocity ranged from 0.2 to 0.4 m/s, with the dominant northward current (Fig. 8). The river mouth area exhibited the highest current velocity, being the narrowest section of the estuary. According to the model results, the maximum current velocity exceeded 0.8 m/s, indicating the significant influence of flood flows typically occurring during the rainy season in the study area. The southern regions near the estuary and along the coast also experienced strong currents, with maximum velocities of 0.5–0.7 m/s. In contrast, the northern coastal areas had smaller, more stable currents because they were less affected by river discharge. Offshore from the estuary, the combined current gradually weakened with increasing distance from the coast due to wave interactions, with maximum velocities between 0.4 and 0.6 m/s. In the offshore zones, where the influence of river current and local topography was minimal, the current speed was weaker, ranging from 0.2 to 0.3 m/s.

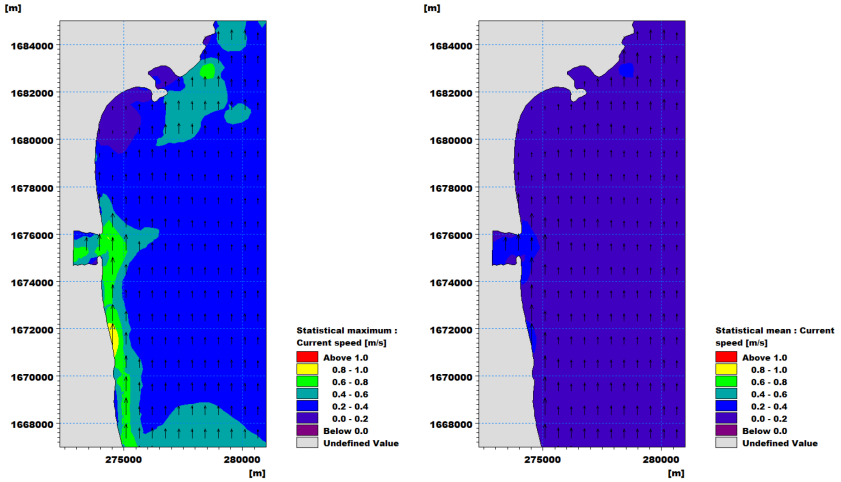

(a) Maximum current velocity (b) Average current velocity

Figure 8. Current field during the Northeast monsoon period

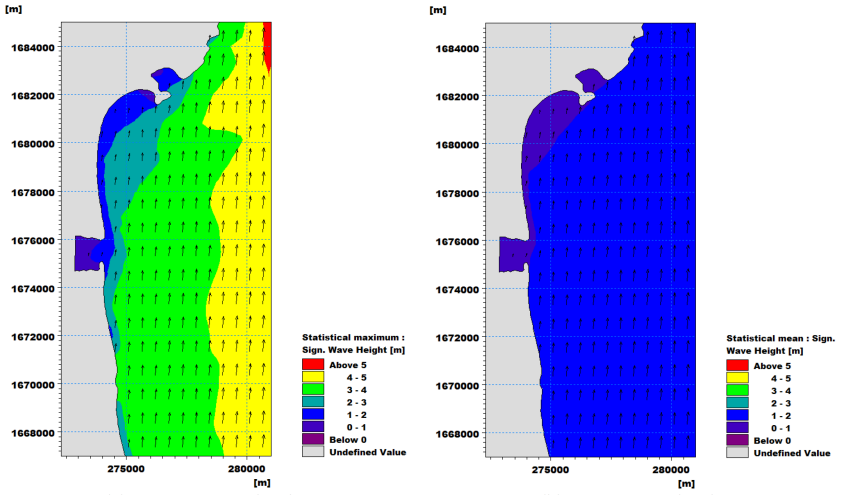

(a) Maximum wave height (b) Average wave height

Figure 9. Wave field during the Northeast monsoon period

During the Northeast monsoon period, the maximum wave height at the estuary area was considerably higher than that observed during the Southwest monsoon period. The dominant wave direction in this period was from the east. In the offshore northeastern region of the study area - directly exposed to the Northeast monsoon and with minimal sheltering - the wave activity was extremely strong, with maximum wave heights ranging from 3.6 to 4.0 m, and in some locations even exceeding 4.0 m. Such conditions pose potential risks to fishing operations in this area. The relatively large wave heights can be explained by the coincidence of the Northeast monsoon season with the rainy and storm season. During the simulation period, the Northeast monsoon winds were particularly strong, with recorded speeds reaching 9.0 m/s [36]. As waves propagate toward the coast, wave heights gradually decrease due to friction with the seabed and the scattering effect. In nearshore and estuarine areas, the maximum wave height decreases sharply, ranging from 1.2 to 2.0 m, and in many nearby regions, only 0.8 to 1.6 m. At the estuary itself, the maximum wave height was below 1.0 m (Fig. 9).

Current and wave characteristics in the Southwest monsoon

Figure 10 illustrates the maximum (Fig. 10a) and average (Fig. 10b) current velocities in the Tra Khuc estuary area during the Southwest monsoon period. The average current velocity in this period is lower than that observed during the Northeast monsoon, ranging from 0.05 to 0.15 m/s, with the dominant current direction from south to north. At the Tra Khuc estuary, all river discharge to the sea and tidal inflow/outflow are forced through a narrow cross-section, resulting in high current velocities in this region. The maximum current velocity at the estuary during this period ranges from 0.2 to 0.4 m/s, with some localized areas reaching 0.4 to 0.6 m/s. Immediately after exiting the estuary into the open sea, due to the combined influence of tides and waves, the current velocity decreases rapidly. The maximum velocity along both coastal sides and offshore areas generally ranges from 0 to 0.2 m/s.

During the Southwest monsoon season, the offshore wave height is significantly smaller compared to that during the Northeast monsoon (Fig. 11). The average wave height in this period ranges from 0.2 to 1.0 m, with the dominant wave direction being southeast. In the offshore area, wave heights are relatively high. For example, in the southeastern part of the study area - where the water depth is greater and directly influenced by southwest or west winds - the maximum wave height ranges from 2.0 to 2.4 m. As waves approach estuaries and nearshore zones, their heights gradually decrease due to scattering, reflection, and coastal depth. Within the Tra Khuc estuary, the maximum wave height is notably reduced, ranging only from 0.4–0.8 m.

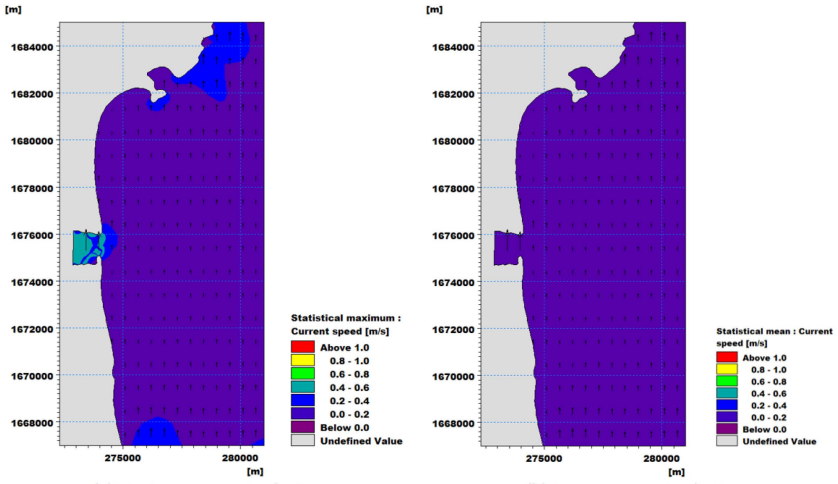

(a) Maximum current velocity (b) Average current velocity

Figure 10. Current field during the Southwest monsoon period

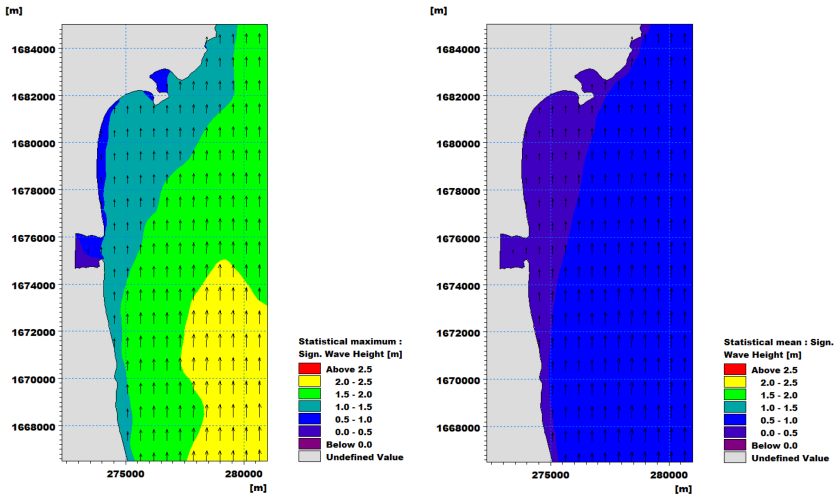

(a) Maximum wave height (b) Average wave height

Figure 11. Wave field during the Southwest monsoon period

Conclusion

This study applied the MIKE 21/3 Coupled Model to simulate the wave and current fields for the Tra Khuc estuary (Co Luy estuary), located in Quang Ngai Province. The model was calibrated and validated using measured nearshore wave and water level data for two periods: September 10–25, 2020, and March 18–25, 2023. NSE and RMSE criteria were applied to assess model accuracy for water level and wave parameters. Most results achieved good performance levels, indicating that the model simulated the hydrodynamic processes with high accuracy and reliability. Two simulation scenarios were developed to analyze the hydrodynamic regimes in the Tra Khuc estuary during the Northeast and Southwest monsoon seasons.

The results show that the average current velocity during the Northeast monsoon was greater than that during the Southwest monsoon. The average current velocity ranged from 0.2–0.4 m/s in the Northeast monsoon and only 0.05–0.15 m/s in the Southwest Monsoon. At the estuary, the maximum current velocity during the Northeast Monsoon exceeded 0.8 m/s, while during the Southwest monsoon, it ranged between 0.2–0.4 m/s, with some areas reaching 0.6 m/s.

Wave height during the Northeast monsoon was significantly higher than in the Southwest monsoon. In the offshore area, the maximum wave height during the Northeast Monsoon ranged from 3.6 to 4.0 m, with some locations exceeding 4.0 m, whereas during the Southwest Monsoon, the maximum offshore wave height was around 2.0 m.

The study successfully identified the characteristics of current and wave fields in the Tra Khuc estuary under two contrasting monsoon conditions. However, it primarily focused on the hydrodynamic aspects, which are fundamental in estuarine and coastal studies. Therefore, further research is needed to deepen the understanding of the mechanisms and impacts of related processes, such as sediment transport, deposition, and erosion along riverbanks. These processes are highly complex and influence not only the stability and morphology of the coastal zone but also the local ecosystems and livelihoods of coastal communities.

Acknowledgments: The authors would like to express their sincere gratitude to the Scientific Research Support Program for Senior Researchers 2025, Project Code: NVCC10.01/25–25, and the Science and Technology Project, Project Code: CT0649.01/21–23, for providing data, partial research results, and financial support to complete this paper.

References

[1] Y. Guo, "Hydrodynamics in estuaries and coast: Analysis and modeling," *Water*, vol. 14, no. 9, 1478, 2022. DOI: 10.3390/w14091478.

[2] K. Amarouche, N. E. I. Bachari, and F. Houma, "Simulation of hydrodynamic behavior using data from coastal weather stations at the Bejaia Bay, Algeria," in *Proc. Euro-Mediterranean Conf. for Environmental Integration*, Bejaia, Algeria, 2017, pp. 1595–1598. DOI: 10.1007/978-3-319-70548-4_463.

[3] H. Rhomad, K. Khalil, R. Neves, J. Sobrinho, J. M. Dias, and K. Elkalay, "Three-dimensional hydrodynamic modelling of the Moroccan Atlantic coast: A case study of Agadir Bay," *Journal of Sea Research*, vol. 188, 102272, 2022. DOI: 10.1016/j.seares.2022.102272.

[4] I. Iglesias, F. A. Buschman, G. Simone, F. Amorim, A. Bio, L. R. Vieira, H. Boisgontier, L. Zaggia, V. Moschino, E. Madricardo, I. Sousa-Pinto, and S. C. Antunes, "Hydrodynamics of a highly stratified small estuary and the influence of nearby river plumes," *Estuarine, Coastal and Shelf Science*, vol. 304, 108843, 2024. DOI: 10.1016/j.ecss.2024.10884.

[5] M. L. Zhang, X. S. Zhu, Y. J. Wang, H. Z. Jiang, and L. Cui, "A numerical study of hydrodynamic characteristics and hydrological processes in the coastal wetlands during extreme events," *Journal of Hydrodynamics*, vol. 35, no. 5, pp. 963–979, 2023. DOI: 10.1007/s42241-023-0072-5.

[6] N. T. Hung, V. D. Cuong, N. T. Thanh, N. V. Hung, and T. Q. Quan, "Modeling of hydrodynamic regimes for the Thuan An estuary," *Journal of Water Management Modeling*, vol. 32, S531, 2024. DOI: 10.14796/jwmm.s531.

[7] K. Hu, P. Ding, Z. Wang, and S. Yang, "A 2D/3D hydrodynamic and sediment transport model for the Yangtze Estuary, China," *Journal of Marine Systems*, vol. 77, nos. 1–2, pp. 114–136, 2009. DOI: 10.1016/j.jmarsys.2008.11.014.

[8] N. T. Hung, D. M. Duc, D. T. Quynh, and V. D. Cuong, "Nearshore topographical changes and coastal stability in Nam Dinh Province, Vietnam," *Journal of Marine Science and Engineering*, vol. 8, no. 10, 755, 2020. DOI: 10.3390/jmse8100755.

[9] N. T. Lam, *Hydrodynamics and morphodynamics of a seasonally forced tidal inlet system*, Ph.D. dissertation, Delft Univ. of Technology (TU Delft), Delft, The Netherlands, 2009.

[10] T. Pang, X. Wang, R. A. Nawaz, G. Keefe, and T. Adekanmbi, "Coastal erosion and climate change: A review on coastal-change process and modeling," *Ambio*, vol. 52, no. 12, pp. 2034–2052, 2023. DOI: 10.1007/s13280-023-01901-9.

[11] M. Armandei, A. C. Linhoss, and R. A. Camacho, "Hydrodynamic modeling of the Western Mississippi Sound using a linked model system," *Regional Studies in Marine Science*, vol. 44, 101685, 2021. DOI: 10.1016/j.rsma.2021.101685.

[12] Z. G. Ji, M. Z. Moustafa, and J. Hamrick, "Hydrodynamic modeling of a large, shallow estuary," *Journal of Marine Science and Engineering*, vol. 12, no. 3, 381, 2024. DOI: 10.3390/jmse12030381.

[13] N. S. Ningsih and M. A. Azhar, "Modelling of hydrodynamic circulation in Benoa Bay, Bali," *Journal of Marine Science and Technology*, vol. 18, no. 2, pp. 203–212, 2013. DOI: 10.1007/s00773-012-0195-9.

[14] J. Gil, A. A. Pires-Silva, and C. J. E. M. Fortes, *Application of the Delft3D system in the modelling of laboratory and field longshore currents*, Delft Univ. of Technology (TU Delft), Delft, The Netherlands, 2006.

[15] P. Parsapour-Moghaddam, C. D. Rennie, and J. Slaney, "Hydrodynamic simulation of an irregularly meandering gravel-bed river: Comparison of MIKE 21 FM and Delft3D flow models," in *Proc. E3S Web of Conferences*, vol. 40, 02004, 2018. DOI: 10.1051/e3sconf/20184002004.

[16] V. Duy Vinh, S. Ouillon, N. Van Thao, and N. Ngoc Tien, "Numerical simulations of suspended sediment dynamics due to seasonal forcing in the Mekong coastal area," *Water*, vol. 8, no. 6, 255, 2016. DOI: 10.3390/w8060255.

[17] J. C. Warner, C. R. Sherwood, R. P. Signell, C. K. Harris, and H. G. Arango, "Development of a three-dimensional, regional, coupled wave, current, and sediment-transport model," *Computers & Geosciences*, vol. 34, no. 10, pp. 1284–1306, 2008. DOI: 10.1016/j.cageo.2008.02.012.

[18] H. S. Lim, C. S. Kim, K. S. Park, J. S. Shim, and I. Chun, "Down-scaled regional ocean modeling system (ROMS) for high-resolution coastal hydrodynamics in Korea," *Acta Oceanologica Sinica*, vol. 32, no. 9, pp. 50–61, 2013. DOI: 10.1007/s13131-013-0352-y.

[19] G. Klonaris, F. Van Eeden, J. Verbeurgt, P. Troch, D. Constales, H. Poppe, and A. De Wulf, "ROMS based hydrodynamic modelling focusing on the Belgian part of the southern North Sea," *Journal of Marine Science and Engineering*, vol. 9, no. 1, 58, 2021. DOI: 10.3390/jmse9010058.

[20] V. T. Nguyen, M. T. Vu, and C. Zhang, "Numerical investigation of hydrodynamics and cohesive sediment transport in Cua Lo and Cua Hoi Estuaries, Vietnam," *Journal of Marine Science and Engineering*, vol. 9, no. 11, 1258, 2021. DOI: 10.3390/jmse9111258.

[21] A. Seenath, "A new approach for handling complex morphologies in hybrid shoreline evolution models," *Applied Ocean Research*, vol. 141, 103754, 2023. DOI: 10.1016/j.apor.2023.103754.

[22] H. L. T. Thanh, V. D. Vinh, and D. P. Tien, "Simulation of typhoon-induced hydrodynamic conditions in the Hai Phong coastal area: A case study of Son Tinh typhoon 2012 and 2018," *Vietnam Journal of Marine Science and Technology*, vol. 24, no. 3, pp. 205–2018, 2024. DOI: 10.15625/1859-3097/18342.

[23] H. B. Thai, D. D. Cham, D. T. Thao, L. D. Hanh, N. T. Son, N. M. Huan, and N. Q. Trinh, "Research on integrated hydrodynamic processes (waves, currents and water levels) by MIKE 21/3 coupled with FM model in the Da Nang coastal zone," *Vietnam Journal of Hydro-Meteorology*, no. 735, pp. 1–11, 2022. DOI: 10.36335/VNJHM.2022(735).1-11. [in Vietnamese].

[24] N. Q. Binh, N. C. Phong, V. H. Cong, and V. N. Duong, "Hydrodynamic modelling for the coastal area of Quang Nam–Da Nang," *The University of Danang Journal of Science and Technology*, vol. 19, no. 1, pp. 19–23, 2021. [in Vietnamese].

[25] N. Q. D. Anh, N. V. Luc, and N. T. Viet, "Numerical simulation of hydrodynamic regime in My Khe Beach, Da Nang City," *Journal of Water Resources & Environmental Engineering*, no. 93(3), 2025. [in Vietnamese].

[26] L. T. Chuong and T. B. Hoang, "The hydrodynamic regime in the estuarine and coastal zones of the Mekong Delta," *Journal of Science and Technology Water Resources*, no. 40, 2017. [in Vietnamese].

[27] V. D. Vinh, T. D. Lan, T. A. Tu, N. T. K. Anh, and N. N. Tien, "Influence of dynamic processes on morphological change in the coastal area of Mekong river mouth," *Vietnam Journal of Marine Science and Technology*, vol. 16, no. 1, pp. 32–45, 2016. DOI: 10.15625/1859-3097/16/1/8016. [in Vietnamese].

[28] X. L. Nguyen, D. T. Dang, and V. Q. Trang, "Simulation of the hydrodynamic field in Nhat Le Estuary, Quang Binh Province," *VNU Journal of Science: Earth and Environmental Sciences*, vol. 37, no. 1, 2021. DOI: 10.25073/2588-1094/vnuees.4460. [in Vietnamese].

[29] N. D. Tuan, N. T. Hung, B. T. Ngan, and V. T. Long, "Application of the 3D hydrodynamic FVCOM model to simulate hydrodynamic regime and thermal structure in the Nhat Le Estuary, Quang Binh Province," *Journal of Science and Technology of Water Resources*, no. 53, 2019. [in Vietnamese].

[30] P. D. Chinh, D. D. Kha, N. T. Sao, N. T. Giang, and D. T. L. Phuong, "Application of MIKE 21/3 FM couple to simulate the hydraulic of Da Nong estuary of Phu Yen province," *Journal of Climate Change Science*, no. 13, 2020. [in Vietnamese].

[31] V. H. Dang, N. H. Lan, N. N. Tien, D. N. Thuc, and N. T. Trang, "Research on hydro-sedimentary and morphodynamic characteristics during the northeast monsoon season in the Cô Tô coastal waters using the MIKE 21/3 FM coupled model," *Journal of Hydro-Meteorology*, no. 634, pp. 28–33, 2013. [in Vietnamese].

[32] N. T. Hung, N. Q. Minh, and V. D. Cuong, "Seasonal changes of hydrodynamic regime at the estuarine and coastal area of Ma River basin," *Vietnam Journal of Science and Technology*, vol. 58, no. 2, 2016. DOI: 10.25073/2588-1102/vjst.58.2.193. [in Vietnamese].

[33] C. D. Dinh, "Effects of hydrodynamical regime on morphological evolution at Cua Dai estuary and coastlines of Quang Nam province,"

Vietnam Journal of Earth Sciences, vol. 42, no. 2, pp. 176–186, 2020. DOI: 10.15625/0866-7187/42/2/15005.

[34] DHI, *MIKE 11, MIKE 21/3 Couple Model FM, User Guide*, DHI, 2021. Copyright by Institute of Geography (now Institute of Earth Sciences), Vietnam Academy of Science and Technology.

[35] T. D. Kieu, L. Q. Huy, and T. T. Tu, "Research on the hydrodynamic regime of the Gianh River estuary, Quang Binh province," *Journal of Science on Natural Resources and Environment*, no. 53, 2024. DOI: 10.63064/khtnmt.2024.628. [in Vietnamese].

[36] European Centre for Medium-Range Weather Forecasts (ECMWF), "Reanalysis data," *Copernicus Climate Data Store*, [Online]. Available: https://cds.climate.copernicus.eu/datasets [accessed: Sep. 20, 2025].